International Journal of Modern Physics B Vol. 3, No. 8 (1989) 1167–1181

FIRST ORDER RAMAN SCATTERING FROM SEMICONDUCTOR QUANTUM DOTS

P.A.M. RODRIGUES, HILDA A. CERDEIRA† and F. CERDEIRA
Instituto de Fisica, Universidade Estadual de Campinas (UNICAMP), 13081 Campinas SP, Brazil

Received 28 February 1989

We develop a model appropriate for describing the Raman spectrum of samples, containing a collection of semiconductor quantum dots with and without dispersion in their linear dimensions. These nanometer size crystallites are assumed to have the same atomic arrangement as that of the bulk material and to be embedded in a host material made up of a different semiconductor of the same crystal structure. The results from our calculations are compared to previous models for polycrystalline materials.

1. Introduction

The recent advent of crystal growth techniques with capability to fabricate artificial semiconductor structures on the nanometer size scale has stimulated interest in quantum confinement of both electronic and vibrational states. There is now considerable theoretical and experimental work on multiple quantum wells i.e., two-dimensional systems fabricated by alternating very thin semiconductor layers of different composition. Confinement of electrons and phonons in these two dimensional layers lead to a variety of interesting phenomena (for reviews see Refs. 1 and 2). It is thus natural to explore the consequences of this confinement in nanostructures of lower dimensionality such as (one-dimensional) quantum wires or (zero-dimensional) quantum dots[3] (QD). There are already several attempts to produce the latter using techniques such as interrupted colloidal growth in solvents[4,5] and particle growth in glasses.[6,7] The effect of confinement of the electronic wave function in these microcrystals appears as a blue shift in the absorption edge.[4–7] However, to the best of our knowledge, the effect of confinement in quantum dots on the vibrational states has not been studied.

In the present work we attempt to describe the changes in the first order Raman spectrum of a typical semiconductor material (of zincblende or diamond type

† Also at International Centre for Theoretical Physics, P.O. Box 586, 34100 Trieste, Italy.

PACS Nos.: 78.30 Fs, 63.20 Dj, 73.20 Dx.

structure) that occur as a consequence of diminishing the particle size to a few lattice constants. For the purposes of the present study, we need to define what we mean by a semiconductor quantum dot.[3] Arbitrarily small structures made up of a given semiconductor material cannot be included in this definition. In small clusters the atoms will seek a more close-packed structure than in bulk crystals. As the number of atoms grow larger, a crossover will take place to the bulk crystalline structure. Recent estimates for Si show that (in vacuum) this crossover should take place for clusters containing $\simeq 10^3$ atoms.[8] However, if the crystallites are embedded in a host material of the same structure as the bulk material, this crossover should occur at smaller sizes. Hence, we shall define our QDs as crystallites made up of a given semiconductor material and having the same atomic arrangement as in bulk (infinite) crystals. The linear dimensions, L, of these crystallites is of the size of a few lattice constants "a", i.e., $L = Na$ with $N \simeq 2$–20. In the case of Si, this means clusters with 64–64,000 atoms. We consider these crystallites to be embedded in a host material of the same structure, but having an optical phonon dispersion such that the optical phonons of the QD cannot propagate into the host material. This situation is analogous to that encountered in GaAs/AlAs superlattices and leads to confinement of the optical phonons[2] within the QD. This confinement will alter the number (and relative intensities) of the peaks in the one-phonon Raman spectrum. We shall study this problem and compare the predictions of our model to other available model for microcrystals[9] that has been applied successfully to ordinary polycrystalline samples and alloy materials.[9–11] First, we review the essential steps leading to the derivation of the Raman cross section[12] for one-phonon process in bulk semiconductor materials (Sec. 2). In Sec. 3, we discuss the modifications necessary to adapt this procedure to the case of a QD. Next (Sec. 4), we show the results of our model and compare these results to that of other models for microcrystalline materials. Finally, in Sec. 5, we offer some concluding remarks.

2. The One-Phonon Raman Spectrum of an Infinite Crystal

In what follows we shall reproduce some essential steps in Loudon's derivation[12] of the Raman cross section for an infinite crystal, in order to determine the modifications that must be introduced for the case of a microcrystal. We consider a Stokes-Raman event in which one photon is scattered from an initial state characterized by frequency (wave vector) ω_i ($\mathbf{K}_i$) into a final state ω_s ($\mathbf{K}_s$) with the creation of one phonon in the μ-th optical branch of wave vector and frequency $\mathbf{q}$ and $\Omega_\mu(\mathbf{q})$ respectively. The electronic system before and after the event remains in the ground state. If by $|a\rangle$ and $|b\rangle$ we denote the initial and final states of the unperturbed system (electron plus phonon plus photon fields, without mutual interaction), the transition probability for this event is given by:

$$\mathcal{W}_{ab} = \left(\frac{2\pi t}{\hbar}\right) \sum_{\mathbf{q}\,\mathbf{k}_s} \left| \sum_{lm} \frac{\langle b|H_I|m\rangle\langle m|H_I|l\rangle\langle l|H_I|a\rangle}{E_{la}\,E_{ma}} \right|^2 \delta(E_{ab}). \tag{1}$$

where,

$$H_I = H_{\text{er}} + H_{\text{ep}} \tag{2}$$

is the interaction Hamiltonian composed of the sum of the electron radiation (H_{er}) and the electron-phonon interaction (H_{ep}) respectively. Using Bloch states of band index n and wave vector $\mathbf{k}$ as a basis for the electronic system, we can express these interaction Hamiltonians in second quantized notation as:

$$H_{\text{er}} = \left(\frac{e}{m}\right)\left(\frac{\hbar}{2\varepsilon_0 \eta V \omega(\mathbf{K})}\right)^{1/2} \sum_{\substack{nn' \\ \mathbf{k}\mathbf{k}'}} C^+_{n'\mathbf{k}'} C_{n\mathbf{k}} \left(a^+(\mathbf{K})\, p^{-\mathbf{K}}_{\mathbf{k}'\mathbf{k}}\, S(\mathbf{k}' - \mathbf{k} + \mathbf{K}) + \text{h.c.}\right) \tag{3}$$

for the electron radiation interaction. In Eq. (3) ε_0 is the permittivity of vacuum, η is the dielectric constant, V the volume of the crystal, $a^+(\mathbf{K})$ ($a(\mathbf{K})$) the creation (annihilation) operator for a photon of frequency ω and wave vector $\mathbf{K}$ and $C^+_{n\mathbf{k}}$ ($C_{n\mathbf{k}}$) the corresponding operators for an electron in a Bloch state $|n,\mathbf{k}\rangle$.

In the above expression explicit use was made of the Bloch function translational property

$$\Phi_{n\mathbf{k}}(\mathbf{r} + \mathbf{R}) = e^{i\mathbf{k}\cdot\mathbf{R}}\, \Phi_{n\mathbf{k}}(\mathbf{r}), \tag{4}$$

where $\mathbf{R}$ is a vector of the lattice, and the electron radiation matrix element:

$$P^{\mathbf{K}}_{\mathbf{k}',\mathbf{k}} = N_0 \int_{v_0} d^3r\, \Phi_{n'\mathbf{k}'}(\mathbf{r})\, e^{i\mathbf{K}\cdot\mathbf{r}}\, \hat{e}(\mathbf{K}) \cdot \mathbf{p}\, \Phi_{n\mathbf{k}}(\mathbf{r}) \tag{5}$$

is integrated over a unit cell of volume v_0 ($V = N_0 v_0$). In Eq. (5) $\hat{e}$ is the polarization vector of the photon and $\mathbf{p}$ is the momentum operator. The function $S(\mathbf{Q})$ in Eq. (3) is a sum over all lattice vectors given by

$$S(\mathbf{Q}) = \frac{1}{N_0} \sum_{\mathbf{R}} e^{-i\mathbf{Q}\cdot\mathbf{R}}. \tag{6}$$

This function has the limiting property

$$\lim_{N_0 \to \infty} S(\mathbf{Q}) = \delta_{\mathbf{Q},0}, \tag{7}$$

modulo a reciprocal lattice vector **G**.

Analogously, we write the electron-phonon interaction (H_{ep}) as:[13]

$$H_{ep} = -iN_0^{1/2}\left(\frac{\hbar}{2\Omega_\mu(\mathbf{q})}\right)^{1/2} T(\mathbf{q}) \sum_{\substack{nn' \\ \mathbf{kk'}}} C^+_{n'\mathbf{k}'} C_{n\mathbf{k}} (b^+_{\mu\mathbf{q}} M^{-\mathbf{q}}_{\mathbf{k}'\mathbf{k}} S(\mathbf{k}' - \mathbf{k} + \mathbf{q}) + \text{h.c.}), \tag{8}$$

where b^+ (b) are creation (annihilation) operators for phonons and:

$$T(\mathbf{q}) = \sum_\nu \frac{U_\nu(\mathbf{q})\hat{e}^\mu_\nu(\mathbf{q}) \cdot \mathbf{q} e^{i\mathbf{q}\cdot\mathbf{x}_\nu}}{M_\nu^{1/2}}. \tag{9}$$

Here the sum is carried over all the atoms in the unit cell. $U_\nu(\mathbf{q})$ is the Fourier component of the ionic potential, $\hat{e}^\mu_\nu(\mathbf{q})$ is the vibrational eigenvector of the phonon with wave vector $\mathbf{q}$ and $\mathbf{X}_\nu$ (M_ν) the position (mass) within the unit cell of the ν-th atom. Finally, the matrix element

$$M^{\mathbf{q}}_{\mathbf{k}'\mathbf{k}} = N_0 \int_{\nu_0} d^3r\, \Phi^*_{n'\mathbf{k}'}(\mathbf{r})\, e^{i\mathbf{q}\cdot\mathbf{r}}\, \Phi_{n\mathbf{k}}(\mathbf{r}) \tag{10}$$

is also integrated over a single unit cell. In Eq. (8) through (10) **k** conservation was assumed and Umklapp processes were neglected.[13,14] Although this procedure is appropriate for an infinite crystal, it is not necessarily valid in a QD. In treating a finite size system, however, we shall use Eq. (8) for the electron-phonon Hamiltonian since, otherwise, we would not be able to obtain an expression for the Raman cross section which is independent of the specific form assumed for this interaction.

Following the Loudon's procedure the scattered light intensity (I_s) is expressed in terms of the incident light intensity (I_i) as:

$$I_s = \frac{I_i}{32\pi^2}\left(\frac{e}{m}\right)^4 \frac{\hbar N_0 \omega_s^3}{c^4 \varepsilon_0^2 \omega_i^2} \sum_{\mathbf{q}} \frac{(n(\mu,\mathbf{q})+1)\, T^2(\mathbf{q})}{\Omega_\mu(\mathbf{q})}$$

$$\times \left| \sum_{\substack{nn' \\ \mathbf{kk'k''}}} \left\{ \frac{P^{\mathbf{K}_s}_{\mathbf{kk''}} M^{\mathbf{q}}_{\mathbf{k''k'}} P^{\mathbf{K}_i}_{\mathbf{k'k}}}{(E_{n'\mathbf{k''}} - E_{n\mathbf{k}}) + \hbar\Omega_\mu(\mathbf{q}) - \hbar\omega_i)\,((E_{n'\mathbf{k}'} - E_{n\mathbf{k}}) - \hbar\omega_i)} + \begin{matrix}\text{five} \\ \text{analogous} \\ \text{terms}\end{matrix} \right\} \right.$$

$$\left. \times\, S(\mathbf{k}' - \mathbf{k} - \mathbf{K}_i)\, S(\mathbf{k}'' - \mathbf{k}' + \mathbf{q})\, S(\mathbf{k} - \mathbf{k}'' + \mathbf{K}_s) \right|^2 \frac{\gamma_0}{(\omega_i - \omega_s - \Omega_\mu(\mathbf{q}))^2 + (\gamma_0/2)^2}, \tag{11}$$

where the finite lifetime of the phonon is taken into account by substituting $\delta(\omega_i - \omega_s - \Omega_\mu(\mathbf{q}))$ by the appropriate Lorentzian function with lifetime broadening γ_0, $n(\mu,\mathbf{q})$ is the Bose population factor for the phonons and c is the velocity of light in vacuum. For infinite crystals ($N_0 \to \infty$), the limiting property of the geometric size function $S(\mathbf{Q})$ (Eq. (7)) reduces Eq. (11) to the well-known expression:

$$I_s = \frac{I_i}{32\pi^2}\left(\frac{e}{m}\right)^4 \frac{\hbar N_0 \omega_s^3}{c^4 \varepsilon_0^2 \omega_i^2} \frac{(n(\mu, \mathbf{q}_0)+1)\, T^2(\mathbf{q}_0)}{\Omega_\mu(\mathbf{q}_0)}$$

$$\times |\overleftrightarrow{\mathscr{R}}|^2 \frac{\gamma_0}{(\omega_i - \omega_s - \Omega_\mu(\mathbf{q}_0))^2 + (\gamma_0/2)^2}, \tag{12}$$

where $\mathbf{q}_0$ is the Brillouin zone center wave vector and the second rank tensor $\overleftrightarrow{\mathscr{R}}$ is given by:

$$\overleftrightarrow{\mathscr{R}} = \sum_{\substack{nn' \\ \mathbf{k}}} \left\{ \frac{P^{\mathbf{K}_s}_{\mathbf{k},\mathbf{k}+\mathbf{K}_i-\mathbf{q}} M^{\mathbf{q}}_{\mathbf{k}+\mathbf{K}_i-\mathbf{q},\mathbf{k}+\mathbf{K}_i} P^{\mathbf{K}_i}_{\mathbf{k}+\mathbf{K}_i,\mathbf{k}}}{((E_{n'\mathbf{k}+\mathbf{K}_i-\mathbf{q}} - E_{n\mathbf{k}}) + \hbar\Omega_\mu(\mathbf{q}_0) - \hbar\omega_i)\,((E_{n'\mathbf{k}+\mathbf{K}_i} - E_{n\mathbf{k}}) - \hbar\omega_i)} \right.$$

$$\left. + \text{five analogous terms} \right\}. \tag{13}$$

3. The One-Phonon Raman Spectrum of a Quantum Dot

As mentioned in Sec. 1, we define a semiconductor quantum dot (QD) as a crystallite which has the same atomic arrangement as in the infinite solid. When the linear dimensions of this crystallite (L) are of the same order of magnitude as same characteristic length (L_c), quantum size effects should become important. This characteristic length is not uniquely defined; it depends on the type of probe used to obtain information about the system.

If we are measuring transport properties L_c should be usually considered of the order of the carrier's mean free path. But it has been by now well established, theoretically[15–17] as well as experimentally in metals[18] and in semiconductors[19–21] that at low temperatures, the phase of the electron wave function remains coherent for distances larger than the mean free path with respect to collisions with impurities. The relevant length becomes $L_\Phi = \sqrt{D\tau_i}$, called the phase-coherence breaking length. Here, D is the diffusion constant and τ_i the electronic lifetime for inelastic scattering events. At finite temperatures $L_c \simeq L_T =$

$\sqrt{hD/kT}$. These systems are called mesoscopic and this character has manifested itself in the form of reproducible aperiodic oscillations in the conductance as a function of external probes.[17,19] This shows that quantum effects in transport properties are probe- as well as sample-dependent. It is therefore reasonable to expect the characteristic length L_c to be different for phonons.

If, as in our case, we are probing the stationary states of the system, this length should be defined in terms of the excitation wavelength (λ) and its dispersion relation, $\Omega(\lambda)$, in such a way that the confinement condition: $n\lambda = L/2$, (n an integer), for a cubic box of side L, produces measurable changes in the energy spectrum. Again, the value of L_c thus defined depends on the type of excitation being considered. In our case we deal with optical phonons of rather weak dispersion and, as we shall see, this leads to values of L_c of very few lattice constants. Expressing the linear dimensions of the crystal as an integral multiple of the conventional cubic unit cell of size a ($L = Na$) we are dealing with $N \simeq 2$–20. For zincblende or diamond-type materials this, in turn, implies in crystallites composed of 64 to 64,000 atoms. The question arises whether such small clusters of atoms will have the same type of atomic arrangement as an infinite crystal. An arbitrarily small structure made up of a given semiconductor material does not satisfy this definition since in this structure the atoms will reorder themselves in a more close-packed arrangement so as to minimize the number of broken bonds. The crossover to bulk structure for Si microcrystals in vacuum has been estimated to take place at $\simeq 10^3$ atoms ($N \simeq 5$).[7] Moreover, if the crystallite is grown embedded in a host material with the same crystallographic structure this crossover might take place at even smaller sizes because of the saturation of surface bonds by host atoms. Hence, it might not be unrealistic to speculate on the effects of quantum confinement on optical phonons in semiconductor quantum dots of these dimensions. Next we discuss the necessary modifications in the derivation of Sec. 2 which lead to the Raman cross section for one-phonon scattering in these QDs.

We assume that the phonon dispersion relation, $\Omega_\mu(\mathbf{q})$, in the QD is the same as that of the bulk crystal. This assumption has been successfully applied to short period superlattices,[2] disordered[11] and amorphous[22] systems and should not be very restrictive. Analogously, the electronic states are assumed to be similar to those in the bulk material, in the sense that they are well described by Bloch states appropriately modified by confinement. The recent calculations of Tomanek and Schlüter[8] lend some support to this hypothesis. Implicit in these assumptions is that surface modes or electron states are not important. These place a more severe limitation in our model than the previous suppositions. Another limiting assumption is keeping for the electron-phonon interaction the same form (Eq. (8)) as for the infinite crystal. There is no justification for this procedure, except that it is the simplest ansatz that leads to a Raman cross section whose general shape is independent of the details of this interaction. We hope, in this way, to obtain the main qualitative aspects of the Raman spectrum of a QD.

With the above assumptions, the Raman spectrum of a QD will be dominated by the functions $S(\mathbf{Q})$ and the condition that the vibrational amplitude of the optical mode vanishes at the crystallite boundary. The latter will depend on the size and shape of the crystallite. Again, in the spirit of obtaining the main qualitative features of the Raman spectrum, we assume cubic microcrystals of linear dimensions $L = Na$. In this case, the only allowed modes are those whose wave vector, $\mathbf{q}$, satisfies:

$$q_i = \frac{\pi n_i}{Na}, (i = x, y, z), \qquad \text{with} \qquad n_i = \pm 1, \pm 2, \ldots, \pm N. \tag{14}$$

Now, the lattice sum $S(\mathbf{Q})$ (Eq. (6)) can be explicitly performed resulting in:

$$S(\mathbf{Q}) = e^{i\theta} \prod_{j=1}^{a} \left[\frac{1}{N} \frac{\sin (Q_j Na/2)}{\sin (Q_j a/2)} \right], \quad (j = x, y, z). \tag{15}$$

The phase factor θ is unimportant since the Raman cross section is defined in terms of $|S(\mathbf{Q})|^2$. Owing to the limiting property of Eq. (7), the function $S(\mathbf{Q})$ is strongly peaked around $\mathbf{Q} = 0$. If we assume the matrix elements in Eq. (11) to be slowly varying functions of $\mathbf{k}$ and we are far away from resonance (i.e., the energy denominators in this equation do not vanish) the summation in this equation can be factorized as:

$$\sum_{\mathbf{k}\mathbf{k}'\mathbf{k}''} \left\{ \cdots \right\} S(\mathbf{k}' - \mathbf{k} - \mathbf{K}_i)\, S(\mathbf{k}'' - \mathbf{k}' + \mathbf{q})\, S(\mathbf{k} - \mathbf{k}'' + \mathbf{K}_s)$$

$$\simeq \sum_{\mathbf{k}} \left\{ \cdots \right\} \sum_{\mathbf{k}'\mathbf{k}''} S(\mathbf{k}' - \mathbf{k} - \mathbf{K}_i)\, S(\mathbf{k}'' - \mathbf{k}' + \mathbf{q})\, S(\mathbf{k} - \mathbf{k}'' + \mathbf{K}_s), \tag{16}$$

where $\{\ldots\}$ refers to the expression in curly brackets in Eq. (11). Within this approximation, it is possible to extend the summations of $\mathbf{k}'$ and $\mathbf{k}''$ to infinity (since $S(\mathbf{Q}) \simeq 0$ for $\mathbf{Q} \neq 0$), in which case it is easy to prove the following exact result:

$$\sum_{\mathbf{k}'\mathbf{k}''} S(\mathbf{k}' - \mathbf{k} - \mathbf{K}_i)\, S(\mathbf{k}'' - \mathbf{k}' + \mathbf{q})\, S(\mathbf{k} - \mathbf{k}'' + \mathbf{K}_s) = S(\mathbf{K}_i - \mathbf{K}_s - \mathbf{q}), \tag{17}$$

with which Eq. (11) reduces to:

$$I_s = C \left| \overleftrightarrow{\mathscr{R}} (\omega_i, \omega_s) \right|^2 \mathscr{L}(N, \omega). \tag{18}$$

Here C is a consant, $\overleftrightarrow{\mathscr{R}}$ is given by Eq. (13) and

$$\mathscr{L}(N, \omega) = N^3 \sum_{\mathbf{q}_n} S(\mathbf{K}_i - \mathbf{K}_s - \mathbf{q}) \frac{\gamma_0}{(\omega - \Omega_\mu(\mathbf{q}_n))^2 + (\gamma_0/2)^2}. \tag{19}$$

Here the summation is performed over all the values of $\mathbf{q}$ allowed by the boundary conditions of Eq. (14). Thus, away from resonance, the shape of the Raman spectrum of a QD is given by the line-shape function $\mathscr{L}(N, \omega)$ of Eq. (19). The same would be true for a sample composed of many quantum dots, all of identical size and shape. If we now consider a sample containing a collection of QDs of identical shapes, but with a random distribution of sizes the Raman intensity would be proportional to

$$I_s(\bar{L}, \sigma, \omega) = \int_0^\infty \mathscr{L}(L, \omega) P_\sigma(L)\, dL, \tag{20}$$

where $P_\sigma(L)$ is a size distribution function with mean value $\bar{L}$ and standard deviation σ.

4. Results and Discussion

In order to obtain the qualitative features of the Raman cross section for our type of systems we must use a concrete function for the optical phonon dispersion relation, $\Omega_\mu(\mathbf{q})$, and give numbers for the different parameters (a, γ_0, etc.) entering into $\mathscr{L}(N, \omega)$ (Eq. (19)). For the dispersion relation we assume isotropy and use the analytic expression which results for a linear chain model.[23] This expression has been used successfully for GaAs and Si.[9,11] Focussing our attention on GaAs as a typical material the line-shape function can be obtained from:

$$\mathscr{L}(N, \omega) = N_0 \sum_{l,m,n=1}^{N} \left(\frac{1}{N_0}\right)^2 \frac{\sin^2(q_x Na/2)}{\sin^2(q_x a/2)} \frac{\sin^2(q_y Na/2)}{\sin^2(q_y a/2)} \frac{\sin^2(q_z Na/2)}{\sin^2(q_z a/2)}$$

$$\times \frac{\gamma_0}{(\omega - \Omega_\mu(\mathbf{q}))^2 + (\gamma_0/2)^2}, \tag{21a}$$

with

$$\Omega_\mu(\mathbf{q}) = [A + (A^2 - 2B\sin^2(qa/2))^{1/2}]^{1/2}$$

$$q = |\mathbf{q}| = \left(\frac{\pi}{Na}\right)(l^2 + m^2 + n^2)^{1/2}; \quad (l^2 + m^2 + n^2)^{1/2} \leq N \tag{21b}$$

where we recall that $N_0 = N^3$ is the number of unit cells and with[24] $A = 4.26 \times 10^4\ \text{cm}^{-2}$, $B = 7.11 \times 10^8\ \text{cm}^{-4}$ and $\gamma_0 = 3.0\ \text{cm}^{-1}$ (from the half width of the in

intrinsic Raman line of bulk GaAs).[11] In Eqs. (21) we have made $\mathbf{K}_i$ $(\mathbf{K}_s) \simeq 0$, an approximation suitable for visible light. The type of Raman spectra predicted by Eqs. (21) for different crystallite sizes are displayed in Fig. 1. In this figure we indicate by $\Omega(X)$ and $\Omega(\Gamma)$ the LO-phonon frequencies for the X and Γ points in the Brillouin zone. The spectrum is seen to consist of several peaks contained in the frequency region between these two extreme values. As the crystallite size increases the spectrum evolves towards a single peak centered around $\Omega(\Gamma)$, which is the Raman spectrum of a bulk crystal. This evolution is very quick and spectra predicted for $L \geq 300$ Å ($N \geq 60$) are essentially identical to those of bulk crystals. Hence, distinctive quantum effects in the Raman spectra of GaAs crystallites are expected only in the range 10 Å $\leq 10^2$ Å.

In order to explore the effects of fluctuations in the crystallite size of real samples, we focus our attention on the spectrum for $N = 8$, which exhibits rich structure. To simulate the effects of a random distribution of crystallites, we

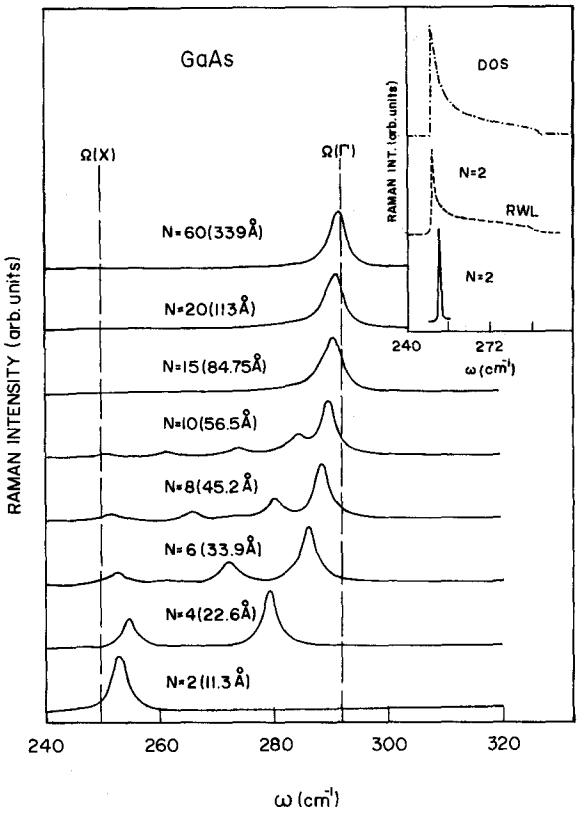

Fig. 1. First order Raman spectra for QDs of linear dimensions $L = Na$ as predicted by our model. Vertical lines indicate LO-phonon frequencies for the Γ and X points of the Brillouin zone. The inset shows the limiting case $N = 2$ for our model (solid curve) and the RWL model (dashed curve) compared to the phonon density of states (dash-dot line).

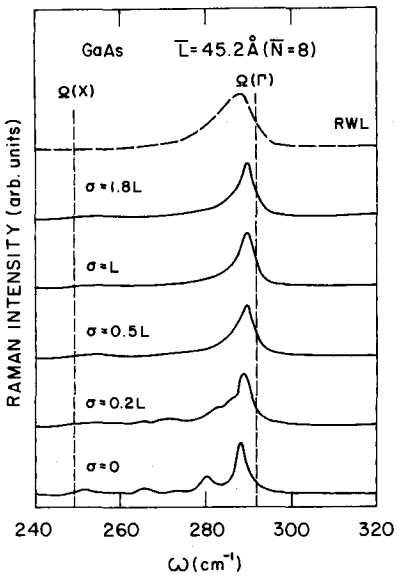

Fig. 2. First order Raman spectra for a sample composed of a collection of QDs of average size $\bar{L} = 45.2$ Å ($\bar{N} = 8$) with a gaussian distribution of sizes having a dispersion σ. The dahsed upper curve shows the prediction of the RWL (Ref. 9) model for the same average crystallite size.

recalculate the Raman cross section (Eq. (20)) using a gaussian distribution of sizes centered about this mean value ($\bar{N} = 8$, i.e. $\bar{L} = 45.2$ Å) and different dispersions σ. The results of this calculation are shown in Fig. 2. We see that the statistical distribution of sizes rapidly smoothes out the Raman spectrum producing, for large enough values of σ ($\sigma \geq \sigma_c$), a single broad and asymmetric peak slightly shifted in frequency from $\Omega(\Gamma)$. Our calculations show that a value of $\sigma_c \cong 35$ Å is enough to produce this effect for any value of $\bar{L}$, as shown in Fig. 3. This is a consequence of the fact that the emitting intensity of a given crystallite is proportional to its volume ($\propto N^3$) and therefore, the Raman spectrum of a given sample is dominated by the contribution of the largest crystallites composing it. This result (single asymmetric Raman peak) is qualitatively similar to the prediction of previous models for microcrystalline samples, such as that proposed by Richter, Wang and Ley[9] (RWL). For the purpose of comparing the predictions for both models, the results of the RWL model for the same crystallite size ($L = 45.2$ Å) are reproduced as a dashed curve in the upper part of Fig. 2. We observe that, in spite of the qualitative agreement, the feature predicted by the RWL model is broader, more asymmetric and exhibits a larger shift towards lower energy from $\Omega(\Gamma)$. The large difference between both models, however, is evidenced when comparing their predictions for samples without size dispersion in the limit $L \to 0$. This limit for both models is shown in the inset of Fig. 1. The density of states of our model solid (based on the dispersion relation of Eq. (21b))

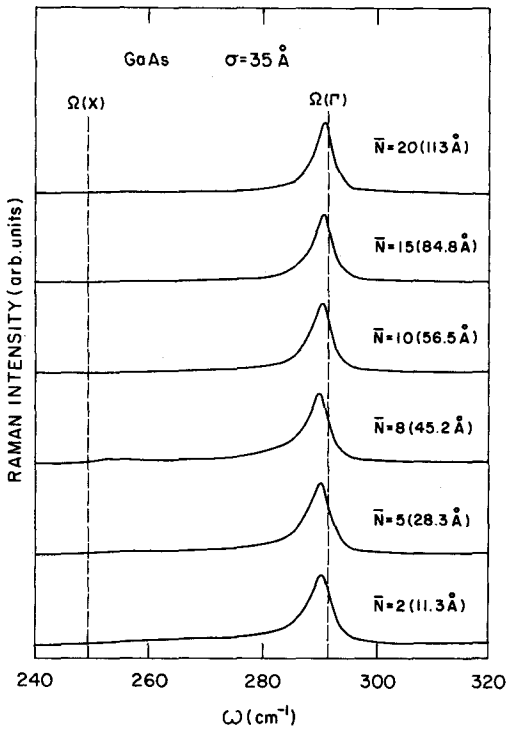

Fig. 3. Raman spectra for QDs with a gaussian size dispersion (σ = 35 Å) and different average crystallite sizes.

is also reproduced there in dash-dotted lines. For this calculation we have taken $\gamma_0 = 0.3\ \text{cm}^{-1}$ in order to better appreciate the limiting predictions of both models. In this limit, our model predicts a single peak of frequency close to $\Omega(X)$, as a consequence of the phonon confinement condition. In contrast, the RWL model in the limit $L \to 0$ ($\gamma_0 \to 0$) predicts a Raman lineshape which essentially coincides with the density of states i.e., the spectrum evolves continuously towards that of an amorphous material[22] as $L \to 0$. Thus, in spite of their apparent similarity for large values of L or considerable dispersion in size distribution, each model applies to two distinct physical situations. Our model is adequate to describe samples composed of mutually isolated QDs, in the definition of Sec. 1, which has as a limit for $L \to 0$ that of a "molecule" of the semiconductor material. The phonons, in this model, are strictly confined within each crystallite. In the RWL model, phonons are localized (with exponentially decaying amplitudes) around regions of crystalline order of size L but these regions are all interconnected by distorted or even amorphous regions of the same material. Hence its smooth transition to the amorphous state as $L \to 0$. A detailed comparison between both models for different crystallite sizes, and for samples of uniform and non-

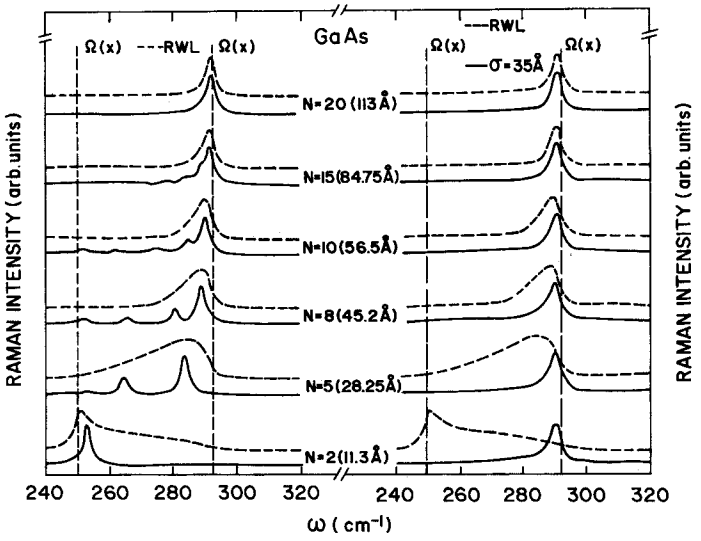

Fig. 4. Raman spectra for different crystallite sizes as predicted by our model (solid lines) and that of Ref. 9 (dashed curves). On the right (left) we assume samples composed of crystallites with a gaussian (uniform) distribution of linear dimensions L having an average value $\bar{L}$ and size dispersion $\sigma = 35$ Å.

uniform size distribution, is shown in Fig. 4 where the features commented above are brought into sharp focus. We believe these differences can be explored as a characterization tool in the early stages of sample production, when both, size dispersion and crystalline perfection are going to be acute quality-control problems. In this respect it is worth to explore further the differences between the Raman spectrum of a random collection of QDs and that of a regular polycrystalline sample. The latter has been well described[9,11] by the RWL model in terms of three parameters readily obtainable from the experimental spectra: (a) the frequency shift $\Delta\omega = \Omega(\Gamma) - \Omega_m$ (where Ω_m is the frequency of the maximum in the observed Raman peak); (b) the total broadening, γ, (full width at half maximum) and (c) the asymmetry, $\rho = \gamma_l/\gamma_h$, defined by the ratio of the half width to lower energies (γ_l) to that at higher energies (γ_h). These parameters are taken directly from the experimental spectrum and their definition is illustrated in the inset of Fig. 5. In this figure we display the dependence of each of these parameters on the crystallite size for the RWL model (dashed curves) and for our model (solid curves) in a sample with a gaussian distribution of crystallite size and a dispersion of $\sigma = 35$ Å. The RWL model predicts more pronounced increases in these parameters as $\bar{L}$ decreases, than our model for a collection of QDs with a random distribution of sizes. Hence, even when the qualitative aspects of the Raman cross sections of the two types of systems described by each model are similar, they differ sufficiently in their detailed quantitative behavior so as to be able to exploit these differences to tell them apart. We thus believe that

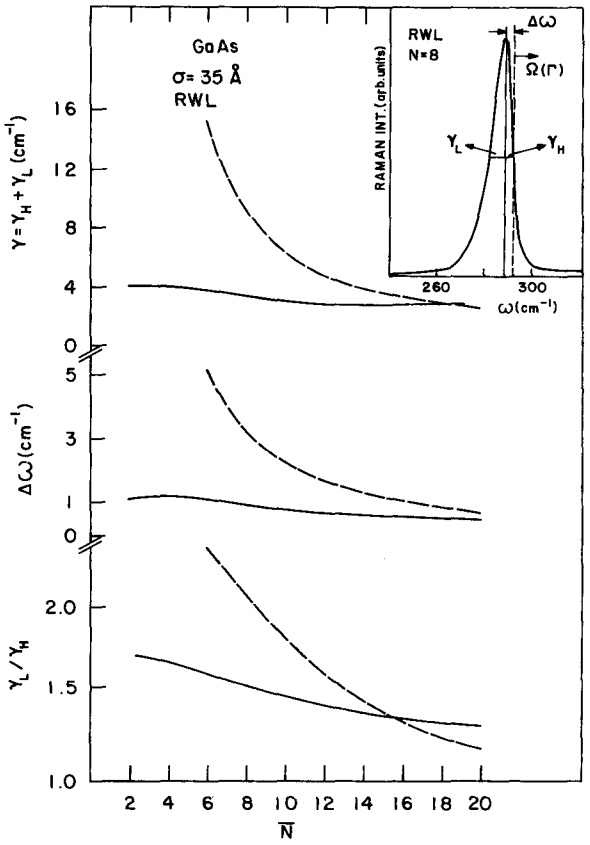

Fig. 5. Comparison between the predictions of our model (for a gaussian distribution of dispersion σ = 35 Å) and that of the RWL model in terms of the line-shape features defined in the inset versus average crystallite size ($\bar{L}$).

analyzing the Raman spectra of microcrystalline samples we should be able to isolate aspects of their average size dependence that distinguish QDs (even when their sizes are not uniform) from other types of polycrystalline samples.

5. Concluding Remarks

In summary, we have developed a theoretical model for the first order Raman spectrum of a sample composed of mutually isolated quantum dots. When the sizes of these quantum dots are uniform their spectra for small crystallites ($L \leq 10^2$ Å) are characteristic and display a multiplicity of peaks due to the combined effects of optical phonon confinement and the relaxation of **k** conservation. The most serious approximations made in order to obtain these results consist of ignoring surface (interface) modes and assuming the same form of

electron-phonon interaction in a QD as in a bulk crystal. When the sample is composed by a collection of QDs with a random distribution of crystallite sizes this structure is washed out. For a gaussian size distribution with dispersion $\sigma \geq \sigma_c \simeq 35$ Å (GaAs), we find that the resulting Raman spectrum consists of a single Raman peak which is asymmetric, broader and downshifted in frequency when compared to the spectrum of the bulk material. This result is qualitatively similar to that predicted by a previous, RWL (Ref. 9), model. However, both models are conceptually different since the RWL does not assume quantum confinement of optical phonons. Rather, it postulates localization, in the form of an exponentially decaying amplitude of the optical phonons in regions of crystalline or average linear dimensions $\bar{L}$. Thus, the RWL model is more adequate to describe the Raman spectrum of a polycrystalline sample which makes a smooth transition to the amorphous state as $\bar{L} \to 0$ than to a collection of QDs of varying sizes. Even for large size dispersion, the detailed quantitative predictions of our model are sufficiently different from those of the RWL model as to suggest that a careful line-shape analysis of the Raman spectrum could be a useful guide to distinguish between these two types of microcrystalline samples.

Acknowledgements

The authors gratefully acknowledge partial financial support from Conselho Nacional de Desenvolvimento Científico e Tecnológico (CNPq), Fundação de Amapro à Pesquisa do Estado de São Paulo (FAPESP) e Financiadora de Estudos e Projetos (FINEP).

References

1. D. S. Chemla, *J. Lumin.* **30** (1985) 502.
2. M. Cardona, in *Lectures in Surface Sciences, Proc. of the Fourth Latin-American Symposium*, (Springer-Verlag, 1987).
3. S. Schmidt-Rink, D. A. B. Miller and D. S. Chemla, *Phys. Rev.* **B35** (1987) 8113.
4. R. Rossetti, S. Nakahara and L. E. Brus, *J. Chem. Phys.* **79** (1983) 1086.
5. R. Rossetti, R. Hull, J. M. Gibson and L. E. Brus, *J. Chem. Phys.* **82** (1985) 552.
6. A. I. Ekimov and A. A. Onushchenko, *Fiz. Tekh. Poluprovodn* **16** (1982) 1215; [*Sov. Phys. — Semicond.* **16** (1982) 775].
7. A. I. Ekimov, Al. L. Efros and A. A. Onushchenko, *Solid State Commun.* **56** (1985) 921.
8. D. Tomanek and M. Schlüter, *Phys. Rev. Lett.* **56** (1986) 1055.
9. H. Richter, Z. P. Wang and L. Ley, *Solid State Commun.* **39** (1981) 625.
10. I. H. Campbell and P. M. Fauchet, *Solid State Commun.* **58** (1986) 739.
11. P. Parayanthal and F. H. Pollak, *Phys. Rev. Lett.* **52** (1984) 1822.
12. R. Loudon, *Adv. Phys.* **13** (1964) 423.
13. P. N. Keating, *Phys. Rev.* **175** (1968) 1171.
14. H. A. Cerdeira, *Solid State Commun.* **12** (1973) 511.
15. B. L. Al'tshuler, V. E. Kratsov and I. V. Lerner, *Zh. Eksp. Teor. Fiz.* **91** (1986) 2276; [*Sov. Phys. JETP* **64** (1986) 1352].
16. P. A. Lee, A. D. Stone and H. Fukuyama, *Phys. Rev.* **B35** (1987) 1039.
17. A. D. Stone, *Phys. Rev. Lett.* **54** (1985) 2692 and references therein.

18. A. Benoit, C. P. Umbach, R. B. Laibowitz and R. A. Webb, *Phys. Rev. Lett.* **58** (1987) 2343; R. A. Webb, S. Washburn and C. P. Umbach, *Phys. Rev.* **B37** (1988) 8455 and references therein.
19. A. B. Kaplan, *Surf. Sci.* **196** (1988) 93.
20. G. Timp, A. M. Chang, J. E. Cunningham, T. Y. Chang, P. Mankiewich, R. Behringer, and R. E. Howard, *Phys. Rev. Lett.* **58** (1987) 2814.
21. A. B. Fowler, A. Hartstein and R. A. Webb, *Phys. Rev. Lett.* **48** (1982) 196.
22. R. Shuker and R. W. Gammon, *Phys. Rev. Lett.* **25** (1970) 222.
23. C. Kittel, *Introduction to Solid State Physics*, 3rd ed., (Wiley, 1967),Chapter 5.
24. J. T. Waugh and G. Dolling, *Phys. Rev.* **132** (1963) 2410.